Isamu OGUMA[1], Ryota GOTO[1], Toshihiko SUGIURA[1]

Keio University (1)

Ultrasonic inspection of an internal flaw in a ferromagnetic specimen using angle beam EMATs

Abstract. *Angle beam EMATs can transmit ultrasonic waves in oblique directions and detect them in a conductive specimen without any contact. Our FEM simulation verified effects of an internal flaw on receiver signal's peaks shown in our experimental results for a ferromagnetic metal. Visualization of displacement distributions obtained by FEM further showed us how ultrasonic waves propagate a circumference of the flaw.*

Streszczenie. *Elektromagnetyczne przetworniki akustyczne (EMPA) mogą transmitować fale ultradźwiękowe w żądanym kierunku oraz wykrywać je bezkontaktowo. Przeprowadzona w pracy symulacja metodą elementów skończonych zweryfikowała możliwość detekcji wewnętrznych wad w ferromagnetyku. (**Badanie ultradźwiękowe wewnętrznych wad w obiekcie ferromagnetycznym za pomocą EMPA**).*

Keywords: Electromagnetic acoustic transducer, Ferromagnetic specimen, Internal flaw
Słowa kluczowe: *Elektromagnetyczny przetwornik akustyczny, obiekt ferromagnetyczny, wada wewnętrzna*

Introduction

It is hoped that quantitative nondestructive evaluation of inner defects in complicated or sophisticated structures such as nuclear power plants, gas pipelines. Among various nondestructive testing methods, ultrasonic testing by EMATs (electromagnetic acoustic transducers) is one of noncontact potential techniques. This technique has been applied and tested in pipelines[1]. There have been quite a few researches on analysis of transmitting and detecting ultrasonic waves in nonmagnetic metals by using EMATs[2, 3]. Some researches of applying EMATs in ferromagnetic metal also have been studied[4, 5]. Researches of EMATs design for good efficiency have also been enhanced[6, 7, 8]. Calculation of magnetostriction and design of EMATs for practical use in various cases were organized[9].

However, there seem few theoretical studies on detection of an internal flaw in a ferromagnetic metal using EMATs. This research aims at FEM analysis of detecting an internal flaw in a ferromagnetic specimen using angle beam EMATs.

Mechanisms of ultrasonic wave generation by EMATs

An EMAT, which consists of a magnet and coils, is a transducer that can detect a flaw in noncontact and nondestructive manner. A.C. current $\boldsymbol{I_\omega}$, flowing in coils, induces eddy current $\boldsymbol{J_\omega}$ on surfaces of the materials, while the magnet generates static magnetic field $\boldsymbol{H_0}$. The cyclic Lorentz force $\boldsymbol{F_\omega}$, generated by $\boldsymbol{J_\omega}$ and $\boldsymbol{H_0}$, produces cyclic displacement $\boldsymbol{u}$, which propagates as ultrasonic waves in the materials. On the other hand, static magnetic field $\boldsymbol{H_0}$ and dynamic magnetic field $\boldsymbol{H_\omega}$ generated by $\boldsymbol{I_\omega}$ produce strains in ferromagnetic metals. These magnetic strains, so-called magnetostriction ε, are changed periodically by resultant magnetic field $\boldsymbol{H_{eff}}$. This magnetostriction ε also generates displacement $\boldsymbol{u}$ and it also propagates as ultrasonic waves in ferromagnetic materials. Fig.1 shows these two types of ultrasonic generation.

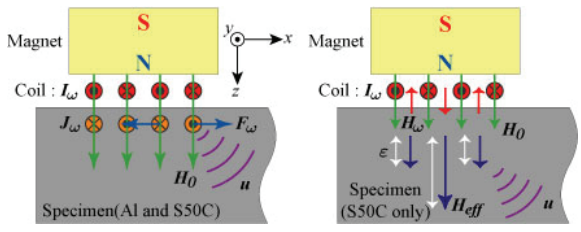

Fig.1. Mechanisms of ultrasonic wave generation by EMATs

The Lorentz forces and magnetostrictive forces

Fig.2 shows our analytical model that is uniform along the y axis so that the model becomes two-dimensional[9].

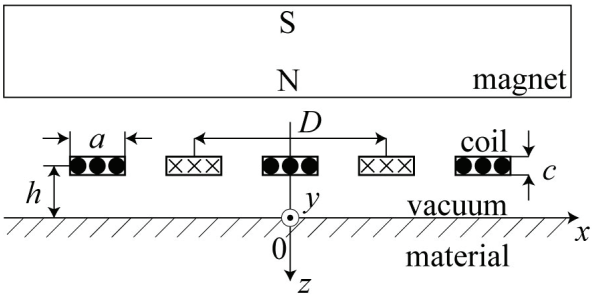

Fig.2. Analytical model

Equations (1) and (2) represent components of the magnetic field generated in a specimen, where a is the coil width, D is the coil pitch, ω is the angular frequency of the coil current, σ is the conductivity of the specimen, μ is the relative permeability of the specimen.

$$(1) \qquad H_x^M = \frac{I}{2a} A_m e^{-k_m h} e^{qz} \cos k_m x$$

$$(2) \qquad H_z^M = \frac{k_m \delta}{\sqrt{2}} \frac{I}{2a} A_m e^{-j\frac{\pi}{4}} e^{qz} \sin k_m x$$

where

$$A_m = \frac{4}{(2m+1)\pi} \sin\left\{\frac{a}{D}(2m+1)\pi\right\}, \quad k_m = \frac{2\pi}{D}(2m+1)$$

$$q^2 = k_0^2 + \frac{2j}{\delta^2} \quad (\mathrm{Re}(q) < 0), \qquad \delta = \sqrt{\frac{2}{\omega\sigma\mu}}$$

The skin depth δ is an important parameter that determines an area where the Lorentz force acts. Since the skin depth has minute order, the relation $H_x^M \gg H_z^M$ holds so that the eddy current density can be approximated as

$$(3) \qquad J_y = \frac{\partial H_x^M}{\partial z} - \frac{\partial H_z^M}{\partial x} \approx \frac{\partial H_x^M}{\partial z}$$

Thus, the Lorentz force can be expressed by

$$(4) \qquad f_x^{(L)} = B_{0z} \frac{\partial H_x^M}{\partial z} = B_{0z} \frac{I}{2a} A_0 q e^{-k_0 h} e^{qz} \cos k_{0x}$$

$$(5) \qquad f_z^{(L)} = -B_{0x} \frac{\partial H_x^M}{\partial z} = -B_{0x} \frac{I}{2a} A_0 q e^{-k_0 h} e^{qz} \cos k_{0x}$$

where B_{0x} and B_{0z} denote the x component and the z component of the magnetic flux density. In ferromagnetic materials, Hooke's law is described as

$$T_I = T_I^{(MS)} + T_I' = -c_{IJ} d_{Jj} H_j + c_{IJ} S_J \quad (I,J = 1,2,\cdots,6; j = x,y,z) \tag{6}$$

where T_I is a component of the total stress, $T_I^{(MS)}$ is a component of magnetostrictive stress, T_I' is a component of the engineering stress, c_{IJ} is a component of elastic modulus, d_{Jj} is a component of piezomagnetic strain coefficients, S_J is a component of the engineering strain. It is substituted to equations (7) and (8) that represent body forces $f^{(MS)}$ caused by magnetostriction,

$$f_x^{(MS)} = \frac{\partial T_1^{(MS)}}{\partial x} + \frac{\partial T_5^{(MS)}}{\partial z} = -\frac{3\varepsilon_t}{H_{0z}} c_{66} \frac{\partial H_x}{\partial z} \tag{7}$$

$$f_z^{(MS)} = \frac{\partial T_5^{(MS)}}{\partial x} + \frac{\partial T_3^{(MS)}}{\partial z} = -\frac{3\varepsilon_t}{H_{0z}} c_{66} \frac{\partial H_x}{\partial x} - 2d_{3z} c_{66} \frac{\partial H_z}{\partial z} \tag{8}$$

where ε_t is magnetostriction. According to equations (1) and (2), gradient of the magnetic field along the z axis is much larger than that along the x axis. This fact with the relation $H_x^M >> H_z^M$ leads to

$$\frac{\partial H_x^M}{\partial z} >> \frac{\partial H_x^M}{\partial x}, \frac{\partial H_z^M}{\partial z} \tag{9}$$

Thus, it brings out that the x component of the magnetostrictive force, $f_x^{(MS)}$, is dominant in this case.

Experimental system

Fig.3 shows our experimental system transmitting and detecting ultrasonic waves by angle beam EMATs. It also shows the route of ultrasonic wave propagation. Here a hole is located inside the specimen as an internal flaw. Parameters such as the input frequency, the coil pitch and the distance between a transmitter EMAT and a receiver EMAT are determined so that the ultrasonic waves can be strongly transmitted in an oblique direction. This system especially excites and detects shear waves. Specimens are an aluminum block and a carbon steel(S50C) block, both of which are 50mm in height, 300mm in width and 100mm in depth.

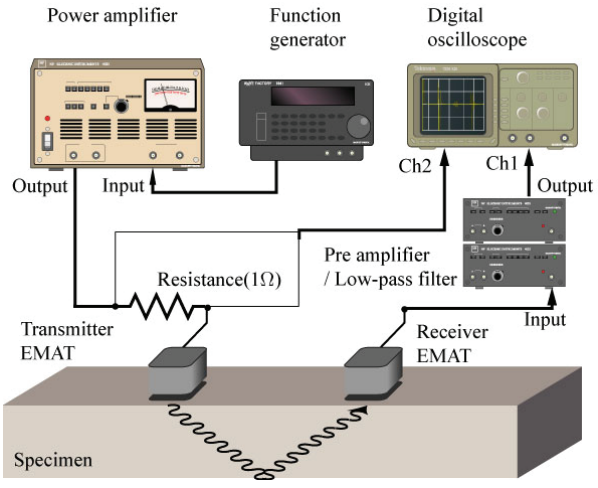

Fig.3. Experimental System

Experimental results

Fig.4 and Fig.5 show a signal detected by the receiver EMAT for each specimen and a result obtained by Wavelet analysis of that signal. The results show that ultrasonic waves propagated in both of the specimens that have no hole. The shear waves arrived at 40 micro seconds through reflection at the bottom of the specimens.

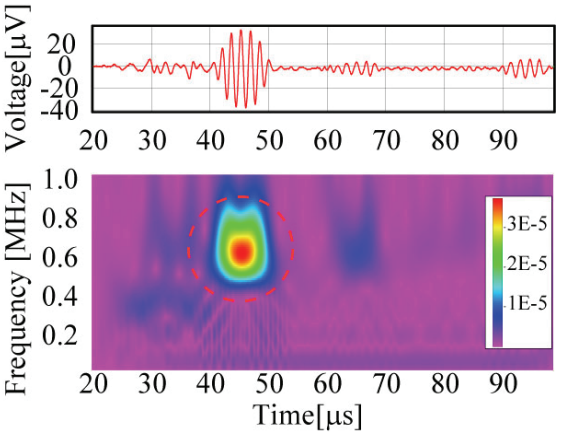

Fig.4. Receiver signals and time-frequency analyses of aluminum

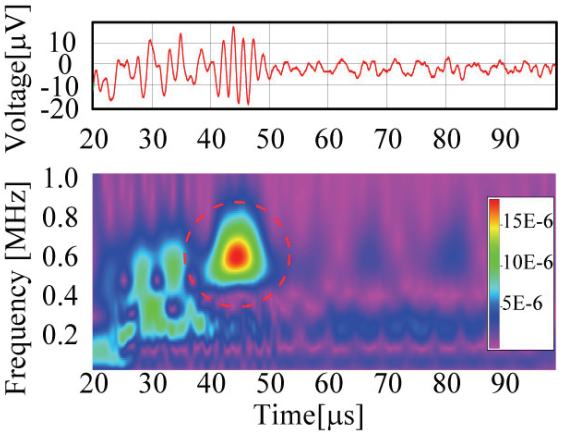

Fig.5. Receiver signals and time-frequency analyses of S50C

Simulation model

Fig.6 shows FEM simulation model.

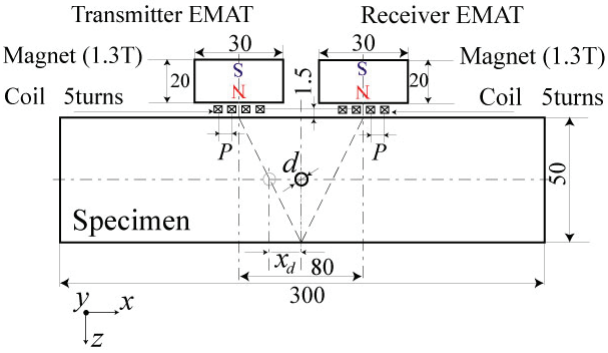

Fig.6. FEM simulation model

The theoretical modeling and formulation can be made for the transmission and detection processes based on elastodynamics and electromagnetics with noncontact and thus clear boundary conditions. The Lorentz forces and the magnetostrictive forces are derived analytically. With the assumption that these forces are concentrated right under the coils, they are evaluated by integrating within the range of the skin depth depending on the material property as following

(10)
$$F_x^{(L)} = \int_0^{\delta}\left(\int_{-\frac{a}{2}}^{\frac{a}{2}} f_x^{(L)}\,dx\right)dz = B_{0z}\frac{I}{ak_0}A_0 e^{-k_0 h}\left(e^{q\delta}-1\right)\sin\frac{ak_0}{2}$$

(11)
$$F_z^{(L)} = \int_0^{\delta}\left(\int_{-\frac{a}{2}}^{\frac{a}{2}} f_z^{(L)}\,dx\right)dz = -B_{0x}\frac{I}{ak_0}A_0 e^{-k_0 h}\left(e^{q\delta}-1\right)\sin\frac{ak_0}{2}$$

(12)
$$F_x^{(MS)} = \int_0^{\delta}\left(\int_{-\frac{a}{2}}^{\frac{a}{2}} f_x^{(MS)}\,dx\right)dz = -\frac{3\varepsilon_t}{H_{0z}}c_{66}\frac{I}{ak_0}A_0 e^{-k_0 h}\left(e^{q\delta}-1\right)\sin\frac{ak_0}{2}$$

The z component of magnetostrictive force plays only a small or negligible role, according to equations (7-9). With these concentrated forces input, FEM simulation is carried out by MSC MARC.

Numerical results

Fig.7 shows time histories of the receiver coil voltage for aluminum and S50C with and without a hole. These results show that if a hole is present, the receiver signal's peaks attenuate and the time of the peaks delays. However, the receiver signal's peaks of experimental results are less than those of FEM simulation because of eddy current loss which is not included in simulation.

Fig.8 shows relations between the position of the hole and the amplitude of the receiver signals. The vertical axis indicates the amplitude of the receiver signals non-dimensionalized by those for specimen without a hole, and the horizontal axis indicates the horizontal distance x_d between the hole and the route of ultrasonic waves. Obtained numerical results show that the receiver signal's peak value changes, depending on the position of the hole. Moreover, attenuation of the signal peaks in the case of a ferromagnetic metal (carbon steel) is larger than that for aluminum. Those results were verified by our experimental results and further imply that mode translational rate by diffraction of waves around a hole in ferromagnetic material is larger than that in nonmagnetic material [10].

Fig.9 shows visualization of displacement around a hole and it represents that ultrasonic waves undergo diffraction around a hole. This diffraction can lead to the signal peak's attenuation and delay in time.

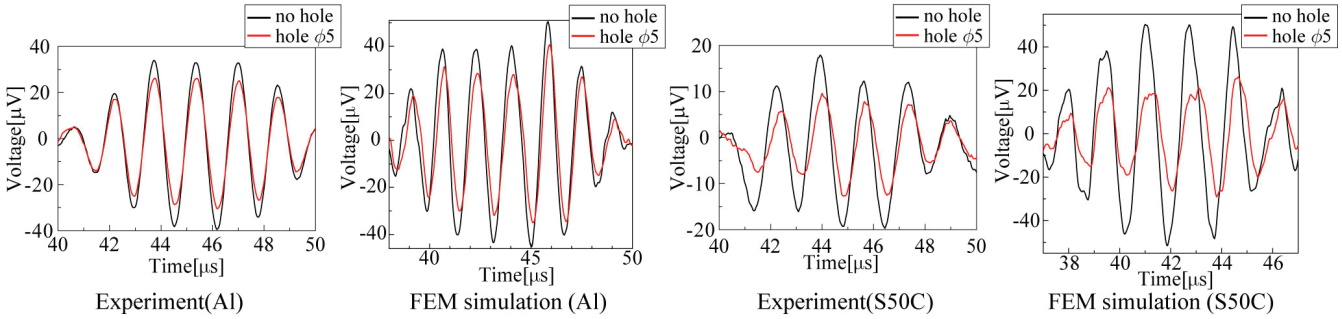

Fig.7. Time histories of receiver coil voltage

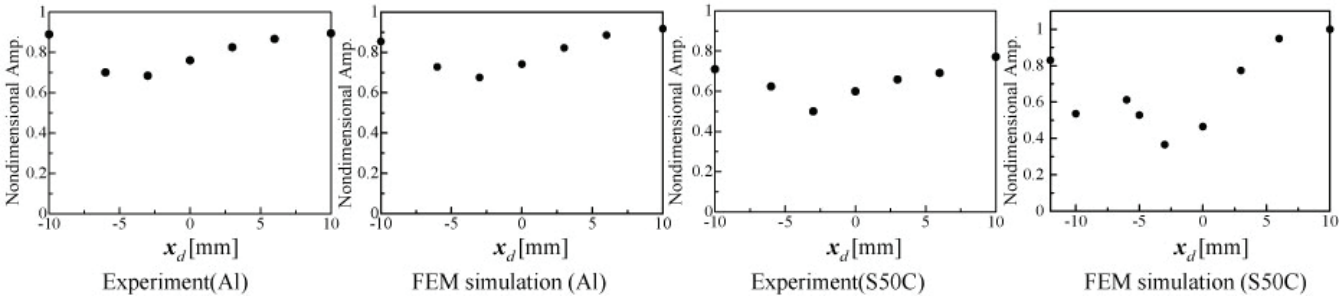

Fig.8. Relations between the position of the hole and the amplitude of the receiver signals

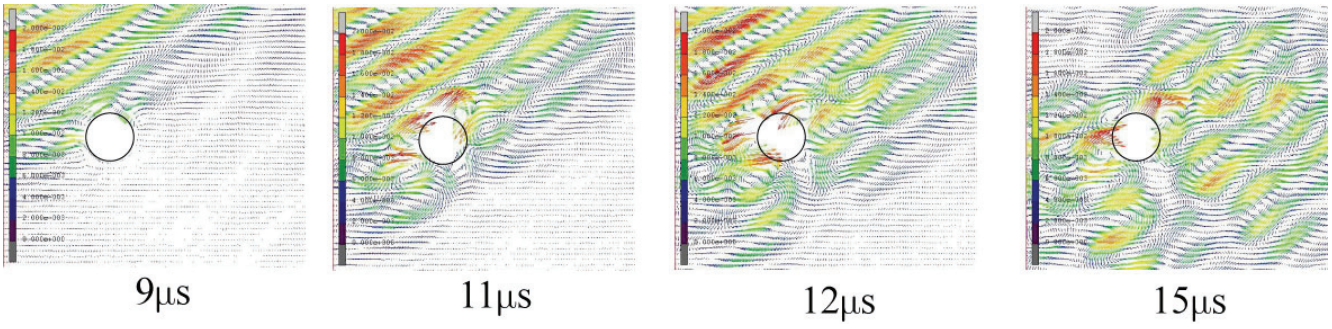

Fig.9. Displacement distributions around a hole

Conclusion

We investigated effect of an internal flaw in a ferromagnetic specimen and in a nonmagnetic specimen under ultrasonic inspection. The above results show important basic features of transmitting and detecting ultrasonic waves and detection of an internal flaw in a ferromagnetic specimen using angle beam EMATs.

Experimental results and FEM simulation results are in qualitative agreement. These results show attenuation of the receiver signal's peak caused by effect of the hole and the fact that the attenuation rate for S50C is larger than that for aluminum. Results of FEM simulation also show appearance of displacement distributions around a hole.

To enhance FEM simulation, we have to consider eddy current loss and reflection rate and mode transformation rate at an internal flaw so that this research suggests the possibility of inverse analysis of an internal flaw.

REFERENCES

[1] Hirao M., Ogi H.: An SH-Wave EMAT Technique for Gas Pipeline Inspection, *NDT&E international*, 32(3), pp.127-132, 1999

[2] Ludwig R., You Z., Palanisamy R.: Numerical Simulation of an Electromagnetic Acoustic Transducer-Receiver System for NDT Applications, *IEEE Transactions on Magnetics*, 29(3), pp. 2081-2089, 1993

[3] Jafari Shapoorabadi R., Konrad A., Sinclair A. N.: Computation of Current Densities in the Receiving Mode of Electromagnetic Acoustic Transducers, *Journal of Applied Physics*, 97(10), pp.1-3, 2005

[4] Thompson R.B.: A Model for the Electromagnetic Generation of Ultrasonic Guided Waves in Ferromagnetic Metal Polycrystals, *IEEE Transactions on Sonics and Ultrasonics*, 25(1), pp.7-15, 1978

[5] Potter R., Schmulian R.: Self-Consistent Computed Magnetization Patterns in Thin Magnetic Recording Media, *IEEE Transactions on Magnetics*, 7(4), pp.873-880, 1971

[6] Huang S., Zhao W., Zhang Y., Wang S.: Study on the Lift-Off Effect of EMAT, *Sensors and Actuators*, 153(2), pp.218-221, 2009

[7] Igarashi B., Alers G.A.: Excitation of Bulk Shear Waves in Steel by Magnetostrictive Coupling, *IEEE Ultrasonics Conference*, 1, pp.893-896, 1998

[8] Wang S., Xin P., Kang L., Zhai G.: Research on Influence of Lorentz Force Mechanism on EMAT's Transduction Efficiency in Steel Plate, *ICIEA*, 5, pp.196-201, 2010

[9] Hirao M., Ogi H.: EMATs for Science and Industry: Noncontacting Ultrasonic Measurements, Boston: *Kluwer Academic Publishers*, 2003, pp.13-38

[10] Miklowitz J.: The Theory of Elastic Waves and Waveguides, Delft: *North Holland Publishing*, 1978, pp.119-152

***Authors**: M. Eng. Isamu Oguma, M. Eng. Ryota Goto, Prof. Toshihiko Sugiura, Department of Mechanical Engineering, Faculty of Science and Technology, Keio University, Hiyoshi3-14-1, Kohoku-ku, Yokohama, Kanagawa, Japan, E-mail: sugiura@mech.keio.ac.jp*.